

An Ultracompact OSNR Monitor Based on an Integrated Silicon Microdisk Resonator

Volume 4, Number 5, October 2012

Ke Xu, Student Member, IEEE

Yimin Chen, Student Member, IEEE

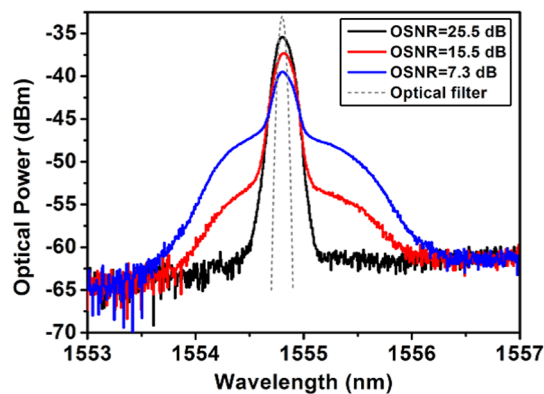
Chao Li

Xia Chen, Member, IEEE

Zhenzhou Cheng, Student Member, IEEE

Chi Yan Wong, Student Member, IEEE

Hon Ki Tsang, Senior Member, IEEE



DOI: 10.1109/JPHOT.2012.2210278

1943-0655/\$31.00 ©2012 IEEE

An Ultracompact OSNR Monitor Based on an Integrated Silicon Microdisk Resonator

Ke Xu, *Student Member, IEEE*, Yimin Chen, *Student Member, IEEE*, Chao Li, Xia Chen, *Member, IEEE*, Zhenzhou Cheng, *Student Member, IEEE*, Chi Yan Wong, *Student Member, IEEE*, and Hon Ki Tsang, *Senior Member, IEEE*

Department of Electronic Engineering, The Chinese University of Hong Kong, Shatin, Hong Kong

DOI: 10.1109/JPHOT.2012.2210278
1943-0655/\$31.00 ©2012 IEEE

Manuscript received June 4, 2012; revised July 19, 2012; accepted July 20, 2012. Date of publication July 25, 2012; date of current version July 31, 2012. This work was supported by the Research Grants Council of Hong Kong under Grant CUHK 416710. Corresponding author: K. Xu (e-mail: kxu@ee.cuhk.edu.hk).

Abstract: Optical signal-to-noise ratio (OSNR) monitoring is essential for control and management of dynamic optical networks. Small footprint, low cost, and less power consumption are always desirable for such monitoring system. In this paper, we demonstrate an integrated dispersion-insensitive in-band OSNR monitor based on a compact silicon microdisk resonator (MDR) with only 5- μm radius. The MDR ($Q \sim 54\,000$) functions as an ultranarrow bandpass filter in the measurement of the OSNR. The monitoring performance is evaluated in a 10-Gb/s return-to-zero differential phase-shift keying (RZ-DPSK) system and is shown to be insensitive to chromatic dispersion from 0 to 850 ps/nm. The input power requirement of the monitor is also studied, which is consistent with the desire for low-power operation. Finally, we analyze the sensitivity of this technique for various Q factors of the MDRs. The results indicate that the sensitivity of this scheme can be improved with higher Q factors.

Index Terms: Optical signal-to-noise ratio (OSNR), silicon photonics, microdisk resonator.

1. Introduction

Optical performance monitoring is an important technique in optical communication systems as it can provide critical information on quality of transmission. Optical signal-to-noise ratio (OSNR) is one of the most important parameters to be monitored for impairment-aware dynamic routing and intelligent compensation, especially in wavelength-division-multiplexed (WDM) reconfigurable optical communication networks, as each channel may route from different path with different amount of accumulated amplified spontaneous emission (ASE) noise. One of the well-established techniques for OSNR monitoring is the polarization-nulling method [1] based on the assumption that the signal is polarized while the ASE noise is unpolarized. However, this technique may not precisely measure the OSNR when the ASE is partially polarized [2] or the signal is depolarized by polarization mode dispersion (PMD) [3]. Another approach is based on uncorrelated beat noise measurements [4], but this scheme exhibits poor dispersion tolerance at high frequency range [5], and it requires the use of a balanced photodiode and a radio frequency (RF) amplifier. A third method is based on interferometry, which is insensitive to data format and dispersion; however, the interference structure makes it not easy to shrink the device footprint [6]–[8]. In addition, quite a few techniques have been demonstrated using optical nonlinear effects, such as four-wave mixing [9],

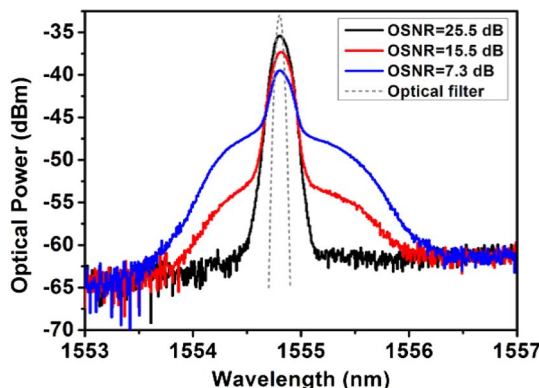


Fig. 1. Principle of OSNR monitoring based on narrow-band optical filter. Black, red, and blue lines represent the spectrum of 10-Gb/s RZ-DPSK with OSNR of 25.5, 15.5, and 7.3 dB, respectively. Dotted line is the passband of an optical filter that filters out a portion of the optical power for OSNR monitoring.

two-photon absorption (TPA) [10], third-harmonic generation [11], and cross-phase modulation [12]. However, relatively high power may be needed in these nonlinear approaches.

In optical networks, it is always desirable to shrink the size and reduce the cost of both optical and electrical components. In the last decade, the technology for photonic devices on silicon-on-insulator (SOI) has advanced considerably and can now be used to make low-cost components for communication systems. The potential to apply the mature and high-yield CMOS nanofabrication technology for integration of optical devices and electronic circuits enables the devices to be fabricated with low cost and large volume. Recently, several silicon waveguide-based OSNR monitoring techniques have been demonstrated, which are potential for monolithic integration [11], [13], [14].

In this paper, we propose an ultracompact OSNR monitor based on a silicon microdisk resonator (MDR). The drop port of the MDR functions as a narrow bandpass filter, which is placed at the center frequency of the signal to extract a portion of the optical spectrum including both signal and in-band noise. For a constant optical power of the signal with different OSNR input to the MDR, the filtered optical power of the channel increases with the in-band OSNR. Yang *et al.* demonstrated that OSNR monitoring was possible in the electrical frequency domain using a 0.25-nm optical filter followed by a 10-GHz photodetector and RF spectrum analyzer [15]. However, electrical spectrum analyzers are rather bulky and expensive instruments. To reduce the device footprint and implementation complexity, we show here that a high-quality factor (Q factor) silicon integrated MDR and a low-speed power meter may be used to measure the OSNR in the optical frequency domain and that the measurement is insensitive to chromatic dispersion (CD). The MDR used in this paper had a radius of only 5 μm . Unlike a fiber-based narrow bandpass filter, it was fabricated by a standard CMOS-compatible process and can be monolithically integrated with an optical receiver, particularly for systems with advanced data formats [16].

2. Principle

For a modulated optical signal, the noise will accumulate as the signal is amplified in the transmission line, and the in-band noise cannot be removed by filters. As illustrated in Fig. 1, the channel's optical spectrum varies with OSNR. The solid line represents the optical spectrum measured by an optical spectrum analyzer (OSA) with 0.1-nm resolution at different OSNR of 7.3, 15.5, and 25.5 dB with a constant input power. As the total power maintains constant and the ratio of signal power to total power is changing with OSNR, the power level at center wavelength will increase with OSNR, as shown in Fig. 1. Thus, the measurement of optical power level at the center frequency can be used to monitor the in-band OSNR. In this paper, we propose and demonstrate the use of a silicon integrated MDR, which functions as an ultranarrow bandpass filter to extract a portion of the signal spectrum and in-band noise around the center frequency shown by the dotted

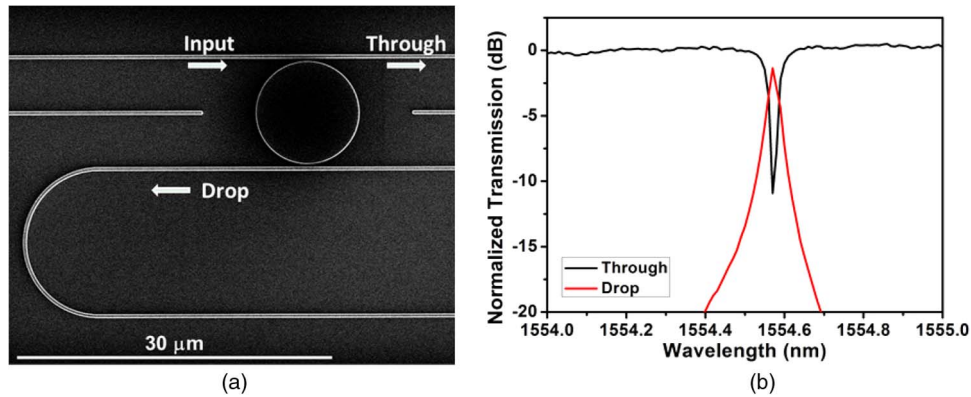


Fig. 2. (a) Top-view SEM image of the silicon microdisk. (b) Measured TE polarized transmission characteristics of the microdisk.

line in Fig. 1. Compared with microring resonator (MRR), MDR can offer higher Q factors, because the waveguide used in the MRR will introduce additional optical loss due to the sidewall roughness from both inner and outer sidewalls, whereas in the MDR, only the loss from the outer sidewall is present. However, MDR is a multimode structure. The number of the whispering-gallery modes (WGMs) can be reduced by shrinking the size of the disk [17], optimizing the structure of the coupling waveguide [18], and designing a ridge planar MDR [19]. Because of the ultranarrow bandwidth of the MDR, the filtered optical power can be used to estimate the in-band OSNR. As this is an optical spectrum measurement, the proposed OSNR monitor is insensitive to either CD or PMD since linear dispersion will not affect the spectra of the signal. It is also compatible with other advanced modulation format such as 8-PSK, QAM, DQPSK, etc. The monitoring sensitivity is dependent on the Q factor of the MDR. The MDR with higher Q can extract the spectrum closer to the center frequency of the signal and thus can provide higher sensitivity.

3. Device Characterizations

The MDR was fabricated on a SOI wafer with a 220-nm-thick top silicon layer and a 2- μm -thick buried oxide layer. The device layout was defined by 193-nm-deep UV photolithography and transferred onto the device layer by dry etching. 750-nm-thick oxide cladding was deposited afterward. A tapered waveguide grating coupler was used to couple light into and out of the MDR. The waveguide width is 350 nm. The radius of the disk is 5 μm , and the gap separation between the disk and the straight waveguides is 250 nm. Fig. 2(a) shows the top-view scanning electron micrograph (SEM) of the MDR. The normalized TE polarized transmission characteristic of the drop port and through port was measured by a narrow-linewidth tunable laser (TL) with 0.01-nm resolution and -10 -dBm optical power, as shown in the inset of Fig. 2(b). The Q factor of the drop port was measured to be $\sim 54\,000$. The insertion loss (fiber-to-fiber) of the drop port is 18 dB, which is dominated by the coupling loss and can be reduced considerably by proper grating coupler design. Growing a thermal oxide as a hard mask can help to further reduce the sidewall scattering loss [20]. It should be noted that the coupling efficiency for TE light is higher than TM. Thus, the coupling efficiency increases with the signal OSNR as the signal is usually polarized and the majority of the ASE noise is unpolarized. We measured the coupling efficiency for signal with an OSNR difference of 25 dB by using an integrated waveguide photodiode. The coupled power for high OSNR is 0.55 dB higher than signal with OSNR of 25 dB lower, which is negligible compared with the proposed monitor sensitivity.

4. Experimental Results and Discussions

OSNR monitoring based on silicon MDR was carried out on a 10-Gb/s return-to-zero differential phase-shift keying (RZ-DPSK) transmission system. As shown in Fig. 3(a), continuous wave (CW)

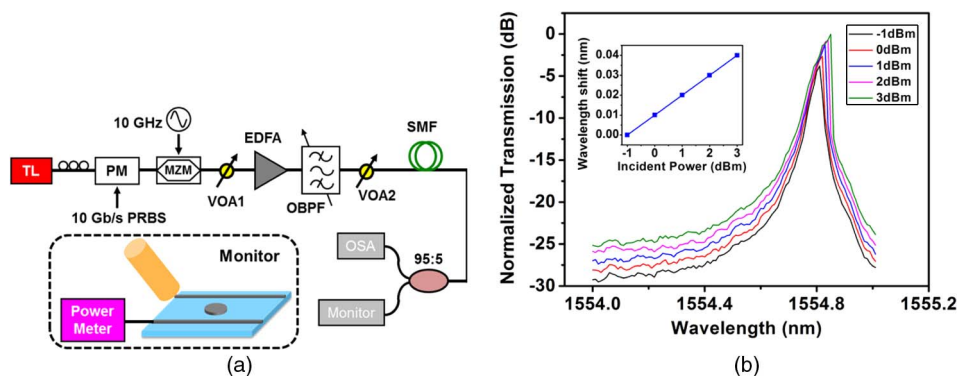


Fig. 3. (a) Experimental setup of OSNR monitoring using silicon microdisk for 10-Gb/s RZ-DPSK system. (b) Optical spectra of MDRs with different incident optical power. Inset: center wavelength shift corresponding to the incident optical power.

at 1554.8 nm from a TL was phase-modulated by a phase modulator (PM) with $2^{31} - 1$ pseudorandom binary sequence (PRBS) and then converted to 35% RZ-DPSK by a Mach-Zehnder modulator (MZM), which serves as a pulse carver. The signal was deliberately degraded by using a variable optical attenuator (VOA 1) to attenuate the signal and an erbium-doped fiber amplifier (EDFA) with a 1-nm optical bandpass filter (OBPF) to induce a controlled amount of band-limited ASE noise. Thus, the OSNR can be varied by VOA 1. The signal was then fed into different lengths of standard single-mode fiber (SMF) with dispersion of 17 ps/nm/km to investigate the dispersion tolerance of the proposed OSNR monitoring scheme. VOA 2 was used for equalizing the attenuation of different lengths of SMF and also ensuring the optical power in front of the SMF is below 0 dBm in order to avoid nonlinear effects in fiber. Then, a small portion (5%) of the signal power was sent into the OSA to verify the OSNR. For the OSNR measurements, a polarization controller (PC) was used to align the polarization of the light to TE direction, and then, the light was coupled into the MDR by the waveguide grating coupler. The filtered optical power was measured by a low-speed power meter.

For a high-Q silicon-based microresonator, the light stored in the cavity may be absorbed via TPA and generate free carriers. This will cause blue shift of resonant wavelength due to free-carrier dispersion (FCD). Besides, TPA-induced free-carrier absorption (FCA) together with surface state absorption may heat up the disk and cause red shift due to thermo-optic effect [21]. Those two effects may initially cancel each other, but red shift will dominate eventually. Thus, the input power should not be too high for a stable operation. As shown in Fig. 3(b), for incident power above -1 dBm, the resonant wavelength of the disk may shift significantly. If the incident power increases to 3 dBm, the resonant wavelength will have a red shift up to 0.04 nm, which is a significant deviation for such a high-Q filter.

On the other hand, the required minimum input power is determined by the sensitivity of the photodetector. The incident power at the input port of the MDR in this experiment is -14 dBm. The insertion loss of the MDR's drop port is ~ 18 dB. Thus, the output power can be easily measured by an integrated silicon germanium photodetector with a typical responsivity of 1 A/W. By reducing the insertion loss of the device, photodetectors with higher sensitivity and bandwidth can be used to lower the required minimum input power and to achieve in-line OSNR monitoring.

For a constant optical power of -14 dBm at the input port of the MDR and the filtered optical power at drop port was measured to be a function of OSNR, as shown in Fig. 4(a). We also investigated the dispersion tolerance of this scheme by employing 0-km [back-to-back (b2b)], 25-km, and 50-km SMFs to introduce different amount of dispersion. It is obvious that the filtered power is not affected by fiber dispersion up to 850 ps/nm/km (50-km SMF), which proves that the proposed OSNR monitoring method is CD insensitive. Insets are the eye diagrams of the b2b RZ-DPSK signals of 10- and 12.5-dB OSNR, respectively. For b2b measurement, the filtered optical power increased from

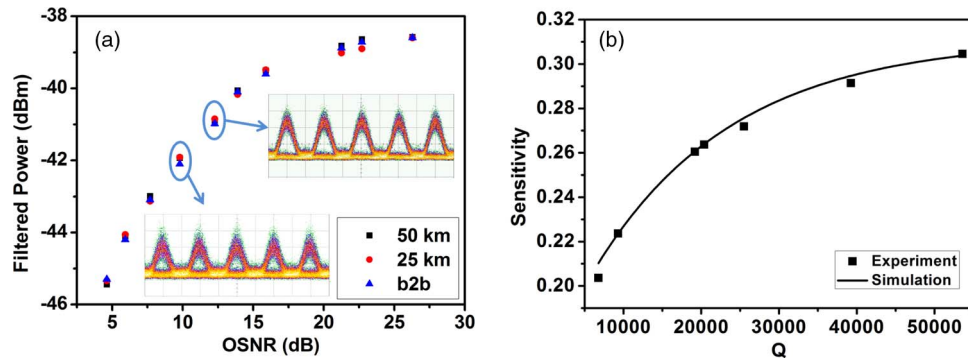


Fig. 4. (a) Filtered optical power as a function of OSNR with different length of transmission fiber. Insets: eye diagram of the degraded b2b signal. (b) The sensitivity of OSNR monitor corresponding to the Q factor of the microdisk.

–45.3 to –38.6 dBm corresponding to OSNR of 4.6 and 26.3 dB, respectively. The filtered power tends to saturate in high OSNR region; however, the scheme provides a sufficient sensitivity (i.e., achieve 5.3-dB filtered power difference) for the OSNR range from 5 to 15 dB, which is of more importance for real applications compared with high OSNR region. For a 10-Gb/s RZ-DPSK system, the required OSNR (bit error rate = 10^{-3}) is 11.1 dB, and the OSNR penalty for 850-ps/nm/km dispersion is 2 dB [22]; thus, it is more important for signal monitoring in a relatively low OSNR range.

The accuracy of optical power measurements in this scheme is quite critical. The input power fluctuation will cause measurement error of the OSNR, especially in high OSNR regime. The power measurement error in our experiment is less than 0.1 dB, which allows for sufficient accuracy of OSNR monitoring. Particularly, in 5–10-dB and 10–15-dB OSNR regime, the OSNR measurement errors are less than 0.16 and 0.24 dB, respectively. Also, it can be seen that dispersion-induced power discrepancy among b2b, 25 km, and 50 km is within the measurement error.

Another critical issue of this technique is to precisely control the filter peak wavelength matched with signal wavelength. The center wavelength of the disk can be thermally tuned by integrated heater [23] or electrically tuned by applying external electrical field [24].

Besides, the Q factor of the MDRs would affect the sensitivity of OSNR monitoring, which may be dependent on the fabrication process and operation environment. This issue is experimentally studied in Fig. 4(b), where the solid line represents to simulation result. For experiment, we utilize several MDRs with different Q to study the filter bandwidth dependence of the monitor sensitivity, which is given by

$$Sensitivity = \frac{P_{max} - P_{min}}{OSNR_{max} - OSNR_{min}}$$

where $OSNR_{max}$ and $OSNR_{min}$ are the measured maximum and minimum OSNR. P_{max} and P_{min} represent the corresponding filtered optical power for maximum and minimum OSNR, respectively. The design parameters of all the MDRs are the same but with different lithography dosage in the fabrication process, which varied the effective gap size in the couplers and thus varied the Q. Fig. 4(b) indicates that the sensitivity increases with the Q factor of the MDR and decreases significantly when the Q drops to below 20 000. Although the sensitivity tends to saturate when the Q is beyond 50 000, further improvement can still be made by higher Q microresonator [20].

It is possible to achieve full integration of the OSNR monitor based on currently available technology. The MDR can be integrated with a PN diode to detect the optical power inside the disk directly [25]. A feedback loop with integrated VOAs, CMOS circuits, and waveguide detectors may be used to control the input power of the optical signal.

5. Conclusion

We have demonstrated an ultracompact OSNR monitor based on an integrated high-Q silicon MDR, which is easy to implement and has the potential for low-cost fabrication and monolithic integration. The footprint of the disk is only about $10\ \mu\text{m} \times 10\ \mu\text{m}$, and it can operate with low power consumption. The scheme was shown to be insensitive to CD and provides a sufficient monitoring range for practical systems. We also demonstrated that the sensitivity can be improved by enhancing the Q factor of the MDR. This method can also be used for communication systems with other advanced modulation format such as DQPSK, 8-PSK, and QAM.

Acknowledgment

The authors thank ePIXfab (www.epixfab.eu) for the device fabrication.

References

- [1] J. H. Lee, D. K. Jung, C. H. Kim, and Y. C. Chung, "OSNR monitoring technique using polarization-nulling method," *IEEE Photon. Technol. Lett.*, vol. 13, no. 1, pp. 88–90, Jan. 2001.
- [2] M. D. Feuer, "Measurement of OSNR in the presence of partially polarized ASE," *IEEE Photon. Technol. Lett.*, vol. 17, no. 2, pp. 435–437, Feb. 2005.
- [3] M.-H. Cheung, L.-K. Chen, and C.-K. Chan, "PMD-insensitive OSNR monitoring based on polarization-nulling with offcenter narrowband filtering," *IEEE Photon. Technol. Lett.*, vol. 16, no. 11, pp. 2562–2564, Nov. 2004.
- [4] W. Chen, R. S. Tucker, X. Yi, W. Shieh, and J. S. Evans, "Optical signal-to-noise ratio monitoring using uncorrelated beat noise," *IEEE Photon. Technol. Lett.*, vol. 17, no. 11, pp. 2484–2486, Nov. 2005.
- [5] M. Bakaul, "Low-cost PMD-insensitive and dispersion tolerant in-band OSNR monitor based on uncorrelated beat noise measurement," *IEEE Photon. Technol. Lett.*, vol. 20, no. 11, pp. 906–908, Jun. 2008.
- [6] X. Liu, Y.-H. Kao, S. Chandrasekhar, I. Kang, S. Cabot, and L. L. Buhl, "OSNR monitoring method for OOK and DPSK based on optical delay interferometer," *IEEE Photon. Technol. Lett.*, vol. 19, no. 15, pp. 1172–1174, Aug. 2007.
- [7] E. Flood, W. H. Guo, D. Reid, M. Lynch, A. L. Bradley, L. P. Barry, and J. F. Donegan, "In-band OSNR monitoring using a pair of Michelson fiber interferometers," *Opt. Exp.*, vol. 18, no. 4, pp. 3618–3625, Feb. 2010.
- [8] J. Schröder, O. Brasier, T. D. Vo, M. A. F. Roelens, S. Frisken, and B. J. Eggleton, "Simultaneous multi-channel OSNR monitoring with a wavelength selective switch," *Opt. Exp.*, vol. 18, no. 21, pp. 22 299–22 304, Oct. 2010.
- [9] S. Cui, L. Li, S. M. Sun, C. J. Ke, and D. M. Liu, "Power transfer function-based dispersion monitoring method applicable to signals with different duty cycles and optical signal-to-noise ratio," *SPIE Opt. Eng.*, vol. 50, no. 7, pp. 075008-1–075008-5, Jul. 2011.
- [10] D. A. Reid, K. Bondarczuk, K. J. Dexter, K. Shi, P. M. Anandarajah, L. P. Barry, W. Hua Guo, J. O'Dowd, M. Lynch, A. L. Bradley, and J. F. Donegan, "Two-photon-absorption-based OSNR monitoring for NRZ-PSK transmission systems," *IEEE Photon. Technol. Lett.*, vol. 22, no. 5, pp. 275–277, Mar. 2010.
- [11] B. Corcoran, C. Monat, M. Pelusi, C. Grillet, T. P. White, L. O'Faolain, T. F. Krauss, B. J. Eggleton, and D. J. Moss, "Optical signal processing on a silicon chip at 640 Gb/s using slow-light," *Opt. Exp.*, vol. 18, no. 8, pp. 7770–7781, Apr. 2010.
- [12] T. D. Vo, M. D. Pelusi, J. Schröder, B. Corcoran, and B. J. Eggleton, "Multi-impairment monitoring at 320 Gb/s based on cross phase modulation radio-frequency spectrum analyzer," *IEEE Photon. Technol. Lett.*, vol. 22, no. 6, pp. 428–430, Mar. 2010.
- [13] B. Corcoran, T. D. Vo, M. D. Pelusi, C. Monat, D.-X. Xu, A. Densmore, R. Ma, S. Janz, D. J. Moss, and B. J. Eggleton, "Silicon nanowire based radio-frequency spectrum analyser," *Opt. Exp.*, vol. 18, no. 19, pp. 20 190–20 200, Sep. 2010.
- [14] K. Xu, H. K. Tsang, G. K. P. Lei, Y. M. Chen, L. Wang, Z. Z. Cheng, X. Chen, and C. T. Shu, "OSNR monitoring for NRZ-PSK signals using silicon waveguide two-photon absorption," *IEEE Photon. J.*, vol. 3, no. 5, pp. 968–974, Oct. 2011.
- [15] J.-Y. Yang, L. Zhang, Y. Yue, V. R. Arbab, A. Agarwal, L. Paraschis, and A. E. Willner, "Optical signal-to-noise ratio monitoring of an 80 Gbits/s polarization-multiplexed return-to-zero differential phase-shift keying channel," *Opt. Lett.*, vol. 34, no. 7, pp. 1006–1008, Apr. 2009.
- [16] C. R. Doerr, N. K. Fontaine, and L. L. Buhl, "PDM-DQPSK silicon receiver with integrated monitor and minimum number of controls," *IEEE Photon. Technol. Lett.*, vol. 24, no. 8, pp. 697–699, Apr. 2012.
- [17] A. Morand, Y. Zhang, B. Martin, K. P. Huy, D. Amans, and P. Benech, "Ultra-compact microdisk resonator filters on SOI substrate," *Opt. Exp.*, vol. 14, no. 26, pp. 12 814–12 821, 2006.
- [18] E. S. Hosseini, S. Yegnanarayanan, A. H. Atabaki, M. Soltani, and A. Adibi, "Systematic design and fabrication of high-Q single-mode pulley-coupled planar silicon nitride microdisk resonator at visible wavelengths," *Opt. Exp.*, vol. 18, no. 3, pp. 2127–2136, Feb. 2010.
- [19] J. F. Song, Q. Fang, X. S. Luo, H. Cai, T.-Y. Liow, M.-B. Yu, G.-Q. Lo, and D.-L. Kwong, "Thermo-optical tunable planar ridge microdisk resonator in silicon-on-insulator," *Opt. Exp.*, vol. 19, no. 12, pp. 11 220–11 227, Jun. 2011.
- [20] M. Soltani, S. Yegnanarayanan, and A. Adibi, "Ultra-high Q planar silicon microdisk resonators for chip-scale silicon photonics," *Opt. Exp.*, vol. 15, no. 8, pp. 4694–4704, Apr. 2007.
- [21] L. W. Luo, G. S. Wiederhecker, K. Preston, and M. Lipson, "Power insensitive silicon microring resonator," *Opt. Lett.*, vol. 37, no. 4, pp. 590–592, Feb. 2012.

- [22] P. J. Winzer and R. J. Essiambre, "Advanced optical modulation formats," *Proc. IEEE*, vol. 94, no. 5, pp. 952–985, May 2006.
- [23] C. Li, J. H. Song, J. Zhang, H. J. Zhang, S. Y. Chen, M. B. Yu, and G. Q. Lo, "Silicon polarization independent microring resonator-based optical tunable filter circuit with fiber assembly," *Opt. Exp.*, vol. 19, no. 16, pp. 15 429–15 437, Jul. 2011.
- [24] K. Xu, G. K. P. Lei, S. M. G. Lo, Z. Z. Cheng, C. Shu, and H. K. Tsang, "Bit-rate variable DPSK demodulation using silicon microring resonators with electro-optic wavelength tuning," *IEEE Photon. Technol. Lett.*, vol. 24, no. 14, pp. 1221–1223, Jul. 2012.
- [25] H. Chen and A. W. Poon, "Two-photon absorption photocurrent in p-i-n diode embedded silicon microdisk resonators," *Appl. Phys. Lett.*, vol. 96, no. 19, pp. 191106-1–191106-3, May 2010.